

Rescue of a Recombinant Machupo Virus from Cloned cDNAs and *In Vivo* Characterization in Interferon ($\alpha\beta/\gamma$) Receptor Double Knockout Mice

Michael Patterson, Alexey Seregin, Cheng Huang, Olga Kolokoltsova, Jennifer Smith, Milagros Miller, Jeanon Smith, Nadezhda Yun, Allison Poussard, Ashley Grant, Bersabeh Tigabu, Aida Walker, Slobodan Paessler

Galveston National Laboratory, Department of Pathology, Sealy Vaccine Center, University of Texas Medical Branch, Galveston, Texas, USA

Machupo virus (MACV) is the etiological agent of Bolivian hemorrhagic fever (BHF), a reemerging and neglected tropical disease associated with high mortality. The prototypical strain of MACV, Carvallo, was isolated from a human patient in 1963, but minimal *in vitro* and *in vivo* characterization has been reported. To this end, we utilized reverse genetics to rescue a pathogenic MACV from cloned cDNAs. The recombinant MACV (rMACV) had *in vitro* growth properties similar to those of the parental MACV. Both viruses caused similar disease development in alpha/beta and gamma interferon receptor knockout mice, including neurological disease development and high mortality. In addition, we have identified a novel murine model with mortality and neurological disease similar to BHF disease reported in humans and nonhuman primates.

A member of the family *Arenaviridae*, Machupo virus (MACV) is an enveloped, bisegmented negative-stranded RNA virus. Arenaviruses utilize an ambisense coding strategy to direct viral gene transcription from two genomic segments, the large segment (L, ca. 7.2 kb) and the small segment (S, ca. 3.3 kb). Each segment carries two viral genes; S encodes the glycoprotein precursor (GPC) and the nucleoprotein (NP), while L encodes the RNA-dependent RNA polymerase (L polymerase) and the small RING finger protein Z. The GPC is posttranslationally cleaved by the cellular site 1 protease into two glycoproteins, GP1 and GP2, and a stable signal peptide (SSP) (1). This peptide is involved in the formation of club-shaped spikes expressed on the virion surface and represents a unique feature of arenavirus GP structure (1–4). The small RING finger protein Z is the counterpart to the matrix protein found in other negative-sense RNA viruses (5). Separating each gene is a noncoding intergenic region (IGR), which acts as a viral mRNA transcription termination region for the viral polymerase (6, 7). At the 5' and 3' ends of each segment are the untranslated regions (UTRs), of which the terminal 19 nucleotides are highly conserved within the *Arenaviridae* family and are believed to be important in efficient viral RNA polymerase binding and transcription.

First isolated during an outbreak in the San Joaquin region of northeast Bolivia, MACV is one of five reported South American arenaviruses capable of causing hemorrhagic disease in humans (8–13). The other viruses include Junin virus (JUNV), Sabia virus (SABV), Guanarito virus (GTOV), and Chapare virus (CHPV). Machupo virus is the etiologic agent of Bolivian hemorrhagic fever (BHF), a disease clinically similar to Argentine hemorrhagic fever caused by JUNV (10, 13–19). The primary route of MACV exposure is believed to be through contact with aerosolized excretions and secretions from the rodent reservoir, *Calomys callosus* (9, 20, 21). Nosocomial transmission of MACV has also been identified following close contact with individuals suffering from the illness (16, 22). In the past 5 years, more cases of BHF have been reported than in the past 40 years combined, all within the San Joaquin region of Bolivia (23–27). Research in the United States utilizing infectious MACV requires a biosafety level 4

(BSL-4) laboratory, and the virus is classified as a select agent by the Centers for Disease Control and Prevention (CDC) and the Animal and Plant Health Inspection Service (APHIS).

Clinically, BHF is a biphasic disease with an estimated incubation time of 3 to 15 days. Symptoms identified in the prodromal phase include fever, headache, vomiting, myalgia, and rash. Severe cases progress into a hemorrhagic/neurological phase in which petechiae, increased vascular permeability, bleeding of the gums, pneumonia, nerve tics, tremors of the tongue and fingers, and coma have been reported. Mortality rates for patients with BHF have been reported at 25 to 35% (28). Convalescence can last weeks to months, with hair loss, weakness, and dizziness reported in most cases. There is no approved therapeutic or vaccine available for MACV. Utilization of immune serum from survivors has been reported in clinical cases, but there have been no published clinical trials to confirm efficacy (16). In animal studies, it has been reported that immune serum can be protective (23, 29, 30). Vaccination with Candid #1, an attenuated vaccine strain of JUNV, has been reported to protect nonhuman primates (NHPs) from a lethal challenge with MACV (31). Candid #1 has been approved for use with BHF in regions of endemicity but has not been approved in the United States or Bolivia (32).

There are no well-established small mammal models for BHF. Adult mice are generally resistant to infection with MACV. Early reports identified suckling hamsters and inbred mice as susceptible following intracranial challenge (9). Recently, STAT-1 knockout mice have been reported to develop an acute and lethal infection following intraperitoneal (i.p.) challenge with MACV (33), highlighting the importance of an intact interferon (IFN) pathway in restricting MACV infection. Guinea pigs have also been re-

Received 4 October 2013 Accepted 20 November 2013

Published ahead of print 27 November 2013

Address correspondence to Slobodan Paessler, slpaessl@utmb.edu.

Copyright © 2014, American Society for Microbiology. All Rights Reserved.

doi:10.1128/JVI.02925-13

ported to succumb to the virus infection through i.p. challenge, but the disease development has not been well characterized (9, 22). Studies utilizing “chaired” NHPs reported lethal disease development following intradermal, intramuscular, and intranasal challenge (34–36). Interestingly, African green monkeys, rhesus macaques, and cynomolgus monkeys developed a lethal late neurological syndrome (LNS), a disease also reported in guinea pig models infected with JUNV (37). A recent publication utilizing mice lacking alpha/beta and gamma interferon receptors (IFN- $\alpha\beta/\gamma$ R^{-/-}) characterized an acute model for lethal disease following challenge with JUNV (38), indicating the critical role of the IFN pathway in limiting JUNV infection in mice. In addition to the neurological involvement identified in serious cases of BHF, both Lassa virus (LASV), an Old World arenavirus and etiologic agent of Lassa fever, and JUNV have been reported to cause different forms of neurological disease in humans and animal models (39–41).

This paper reports, for the first time, the development of a reverse genetics system and successful rescue of a pathogenic recombinant MACV (rMACV Carvallo, the prototypical strain). The rescue of an rMACV will ensure a genetically well-characterized virus stock and will enable us to study the biology of MACV in greater detail. The reverse genetics system will also facilitate the rational design of an experimental MACV vaccine. During the development of this system, we also generated a minigenome (MG) reporter system, which allowed us to study the *cis*- and *trans*-acting factors required for MACV replication and gene expression in a BSL-2 environment without select agent restrictions, therefore enhancing our capabilities for potential virus replication studies and drug screening. And finally, we have identified a novel murine model of MACV-induced LNS, similar to what is described in reports of infected humans and NHPs (34–36). This is the first reported model of LNS in a murine species infected with a New World arenavirus.

MATERIALS AND METHODS

Cells, viruses, and biosafety. Baby hamster kidney (BHK-21) and Vero cells (American Tissue Culture Collection) were maintained in Dulbecco's modified Eagle's medium supplemented with 10% fetal calf serum and L-glutamine. The wild-type Carvallo strain of MACV (GenBank accession numbers JN794583.1 and JN794584.1) was obtained from Thomas G. Ksiazek (University of Texas Medical Branch [UTMB]). Viral working stocks of the wild-type and recombinant viruses were generated by infecting Vero cells (multiplicity of infection [MOI] = 0.01 PFU/cell) and collecting virus-containing tissue culture supernatant (TCS) at 96 h postinfection (hpi). Cellular debris was eliminated from the TCS through centrifugation, and the viruses were concentrated and purified through Ultra 100K Filter Devices (Ultracell 100K centrifugation filter; Amicon) to remove cellular factors that may affect the immune response. All work with infectious MACV and rMACV was performed in the UTMB BSL-4 facility in accordance with institutional and safety guidelines.

Sequencing of full-length S and L genomic RNAs from MACV Carvallo strain. RNA (0.5 to 1.0 mg) was isolated by an RNA purification kit (DNA-Free RNA kit, R1014; Zymo Research) at 96 hpi from MACV-infected Vero cells. Viral cDNA was synthesized by reverse transcription (RT) using either virus-specific primers or random primers. Virus-specific primers complementary to S and L genome RNAs were used to generate cDNA fragments of each segment. The entire S and L segments were amplified in three and five DNA fragments, respectively, by PCR. PCR products were gel purified (Zymoclean Gel DNA recovery kit, D4001; Zymo Research) and directly sequenced to obtain the corresponding master sequences for the MACV S and L genome RNAs. To confirm the

sequences of these amplified DNA fragments, a second RT reaction was performed using random primers to generate cDNA. This cDNA was then amplified utilizing the same primers as described above to amplify the S and L segments. Sequencing data were analyzed using the program Clone Manager V9.

Determination of 5' and 3' termini of both S and L segments. To determine the sequences of the 5' and 3' 19-nucleotide terminal regions of the S and L segments, total RNA was isolated from Vero cells infected with MACV. RNA was treated with RNA 5' Tobacco acid pyrophosphatase (Epicentre) and ligated using T4 RNA ligase I as previously described (42). The ligated RNA was reverse transcribed utilizing the primers MACV_SsegR312 (5'-AGGGTGACTGACTGGAATC-3') and MACV_SsegF3129 (5'-GACA TGAGCCTATCCACTTC-3') and the primers MACV_LsegR349 (5'-TGTG ATGGATGTCGGTAGTG-3') and MACV_LsegF6917 (5'-AGGCGTGTGC TTCACAGGAC-3') for the S and L segments, respectively. The cDNA was used for amplification through PCR utilizing the same primers. Fragments were gel purified and sequenced.

Construction of plasmids for MACV reverse genetic systems. To generate the pBSII-S vector plasmid containing the full-length antigenomic sense MACV S segment, two fragments derived from the S segment with overlapping restriction sites were amplified by PCR. The cDNA fragments were then digested and ligated into the vector pBlueScript (pBSII). The vector pBSII-L plasmid containing the L segment was generated in a similar manner using three cDNA fragments. The segments were digested from the cloning vector plasmids and inserted in antigenomic orientation into the murine Pol-I-driven pRF42 mPol-I-expressing plasmid to generate pPol-I-MACVSag and pPol-I-MACVLag plasmids, which expressed the full-length viral S segment genomic RNA and L segment genomic RNA, respectively. A silent G-to-A mutation at nucleotide 1991 within N gene was introduced into the S segment as a genetic marker for the recombinant MACV. To express the MACV NP and L protein in *trans*, MACV NP and L genes were cloned into the Pol-II-driven mammalian gene expression plasmid pCAGGS to generate plasmids pPol-II-NP and pPol-II-L, respectively. An RsrII restriction site was added to the 5' end of primers corresponding to the ATG codon of each gene and was utilized for digestion and ligation of the gene segments into the plasmids. The L polymerase gene was inserted into pCAGGS by three DNA fragment ligation (pPol-II-L), while the NP was directly inserted as a single fragment (pPol-II-NP). Sequences of all plasmids were confirmed by sequence analysis. Detailed cloning method information is available upon request.

MACV minigenome systems. The plasmids expressing MACV L and S segment MG were generated as described previously (42). Briefly, viral genes on the pPol-I-MACVSag and pPol-I-MACVLag template plasmids were replaced by the green fluorescent protein (GFP) and firefly Luciferase (fluc) reporter genes (see Fig. 2A). BHK-21 cells (6×10^4 /well in a 12-well plate) were transfected with 0.5 μ g of pPol-II-NP, 0.5 μ g of pPol-II-L, and 0.5 μ g of plasmid expressing MACV L or S MG segments as indicated. At 3 days posttransfection, cellular lysate was collected and the bioluminescent signal was assayed, utilizing a luciferase reporter assay kit (Promega E1500 or E1910) for luciferase expression.

Rescue of rMACV. The rescue of rMACV was completed in a manner similar to that described previously by our laboratory (42). Briefly, equimolar amounts of the two full-segment MACV plasmids and the two expression plasmids were transfected into BHK21 cells. Supernatant from these cells was collected at 4 days posttransfection. A single passage in Vero cells was performed to generate a higher-titer stock of rMACV. The rMACV sequence, including the introduced G1991A gene tag within the NP gene, was confirmed by whole genomic sequence analysis.

Virus growth kinetics. To determine viral growth kinetics, Vero and A549 cells were infected at an MOI of 0.01 and TCS was collected from 0 to 4 days postinfection (dpi). Plaque assay titrations were completed as previously described (42).

Animal experiments. Six- to 8-week-old IFN- $\alpha\beta/\gamma$ receptor double knockout (IFN- $\alpha\beta/\gamma$ R^{-/-}) mice on a C57BL/6 background and wild-

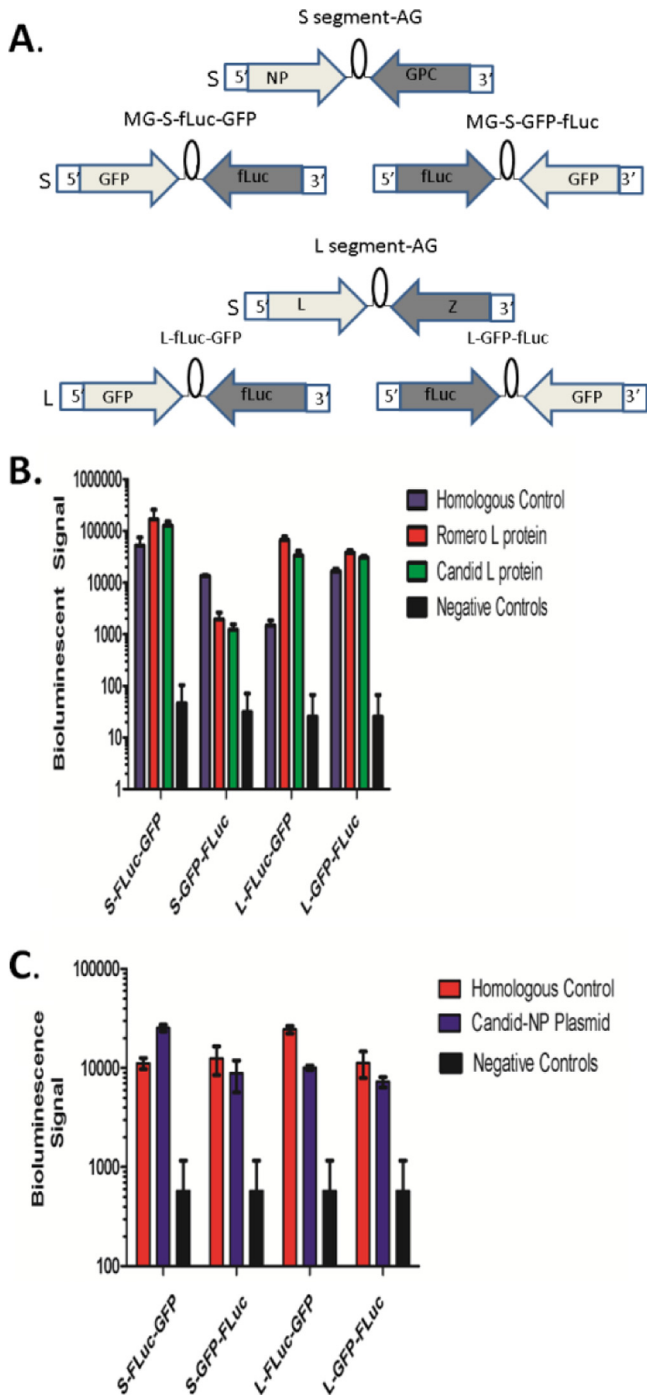


FIG 2 Minigenome (MG) reporter system for MACV. (A) Graphical representation of four MACV minigenome reporter plasmids. The MACV S and L antigenomic RNAs are shown (S segment AG and L segment AG, respectively). Four MACV MG reporter plasmids (S-fluc-GFP, S-GFP-fluc, L-fluc-GFP, and L-GFP-fluc) were generated with fluc and GFP genes replacing viral genes in the S and L segments while leaving the UTR and IGR in place. (B) MACV MG-driven fluc expression in BHK cells cotransfected with one of the MACV MG reporter plasmids as indicated and the MACV NP-expressing plasmid. To provide the L protein in *trans*, cells were simultaneously transfected with the MACV L protein-expressing plasmid (homologous control), the JUNV L-expressing plasmid (Romero L protein), or the Candid #1 L-expressing plasmids (Candid #1 L protein), respectively. In the negative-control samples, cells were transfected with MG reporter plasmids without NP or

of the S segment for sequence [JN794584](#). Comparisons of our sequencing results to another set of reported MACV sequences ([AY619643](#) and [AY619642](#)) demonstrated the exact same four nucleotide differences ([Fig. 1A](#)), which were also reported in the sequences of JUNV (GenBank accession numbers [AY619641](#) and [AY619640](#)) by other groups and were determined to be not viable for the rescue of an infectious virus ([42](#)). There were two additional nucleotide differences at positions 6 and 8 at the 5' end of the L segment between [AY619642](#) and the sequence determined herein ([Fig. 1A](#)).

Development of the Machupo virus minigenome to identify the *trans*-acting factors required for efficient RNA replication and transcription. To confirm whether the 5' and 3' UTRs of MACV identified in this study were functional for virus RNA replication and transcription, we developed a MACV minigenome system. Minigenome reporter plasmids were generated containing the full UTRs and IGRs of MACV S and L segments with viral genes replaced by either fluc or GFP reporter genes ([Fig. 2A](#)). Plasmids expressing MACV L and NP in *trans* were generated by inserting viral NP and L protein genes into a Pol-II-based expression vector (pCAGGS, pPol-II-NP, and pPol-II-L). Results from our MG experiment ($n = 3$ for each reporter plasmid) confirmed that the homologous MACV L and NP provided in *trans* were sufficient to support MACV minigenome RNA replication and transcription ([Fig. 2B](#)). These results also confirmed the functionality of the UTRs identified in this study. MG-driven fluc reporter gene expression was substantially stronger for all MG constructs in the presence of NP and L protein than for samples transfected with the corresponding MG reporter plasmids only.

To further test the compatibility of the MACV MG template with heterologous NP or L proteins derived from other New World arenaviruses, we tested the relative efficiencies of NP and L proteins of MACV, JUNV Romero, and Candid #1 vaccine strains in supporting MACV minigenome replication. We chose the JUNV Romero and Candid #1 strains as they are genotypically similar to MACV. Sequencing comparison of published JUNV virus sequences (GenBank accession numbers [AY619640](#), [AY619641](#), [AY746353](#), and [AY746354](#)) to MACV (GenBank accession numbers [JN794583](#) and [JN794584](#)) identified a 69% and 72% nucleotide similarity for the L and S segments, respectively. Amino acid similarities between the virus segments were 73% and 87% for the L and S segments. The rationale for this experiment is to potentially attenuate MACV in the future by introducing genes from the JUNV vaccine strain.

Analysis of the MACV minigenome-driven fluc expression confirmed that the L proteins of both JUNV and Candid #1 were compatible with MACV NP in supporting MACV minigenomic RNA replication and transcription ([Fig. 2B](#)). Further analysis indicated that Candid #1 NP could replace MACV NP and could efficiently support MACV MG template replication in the presence of MACV L protein ([Fig. 2C](#)). These data clearly showed that

L protein expression plasmids. (C) MACV MG-driven fluc expression in BHK cells cotransfected with one of the MACV reporter plasmids and the MACV L protein expression plasmid. To provide NP in *trans*, BHK cells were also transfected with the MACV NP-expressing plasmid (homologous control) or the Candid #1 NP-expressing plasmid (Candid#1-NP plasmid). In the negative-control samples, cells were transfected with MG reporter plasmids without expression plasmids for NP or L protein. Each experiment was completed in triplicate; error bars represent standard deviations (SD).

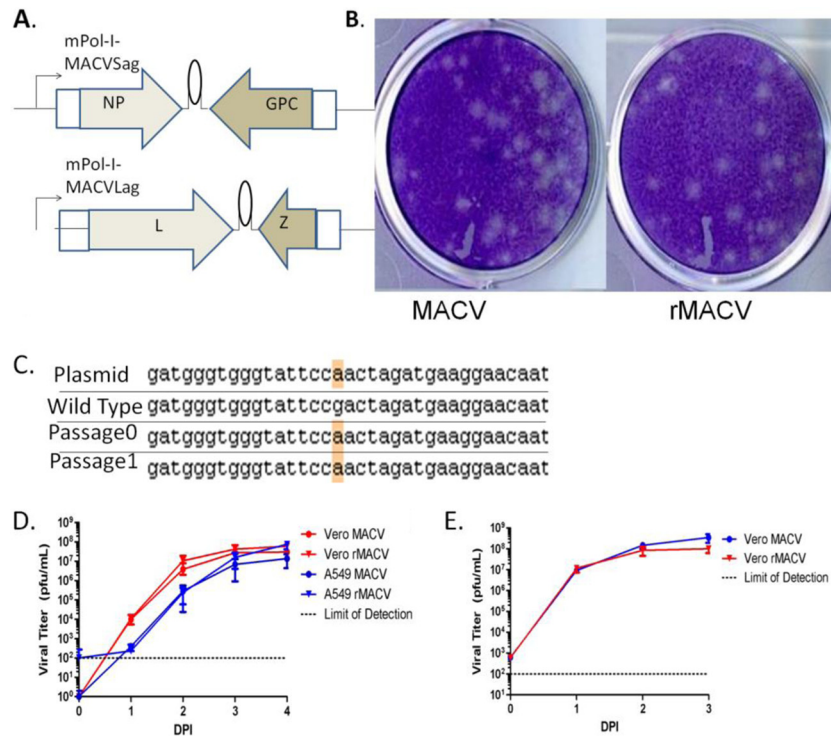


FIG 3 Rescue of rMACV. (A) Graphical representation of plasmids expressing the MACV antigenomic S and L RNAs used for the reverse genetics system. (B) Plaques formed by MACV and rMACV on Vero cells at 8 dpi. Plaque size and morphology are similar for the two viruses. (C) Sequencing of rMACV confirmed the single genetic marker introduced into the original plasmid that differentiates rMACV from MACV. (D) Multiple-step growth curve of MACV and rMACV in Vero cells and A549 cells (MOI = 0.01). (E) One-step growth curve of MACV and rMACV in Vero cells (MOI = 1). Data shown are the averages of three experiments \pm SD.

the NP and L protein of JUNV could replace their MACV counterparts in the MG systems, suggesting the feasibility of rational design of an MACV vaccine candidate by introducing a heterogeneous NP or L gene from the attenuated JUNV into MACV genome.

Rescue of recombinant Machupo virus and *in vitro* characterization. To generate rMACV from cloned cDNA plasmids (Fig. 3A), we transfected BHK cells with equimolar concentrations of pPol-I-MACVSag, pPol-I-MACVLag, pPol-II-NP, and pPol-II-L plasmids. TCS was collected at 96 h posttransfection, and the virus titer was 8×10^4 PFU/ml. To generate a working stock with higher virus titer, we infected Vero cells at an MOI of <0.01 to avoid the potential formation of defective interfering particles. TCS was harvested at 96 hpi and purified according to the manufacturer's protocol (Millipore Amicon Ultra Centrifugal Filters 100K, UFC910096). Whole-genomic RNA sequence analysis of rMACV confirmed no additional mutations other than the genetic marker introduced to the rMACV genome RNA (Fig. 3C). Plaques formed by both viruses on Vero cells at 8 dpi were similar in their morphology and size (Fig. 3B). rMACV and MACV demonstrated very similar growth curves in A549 cells at an MOI of 0.01 and in Vero cells at MOIs of 0.01 and 1 (Fig. 3D and E), indicating that the rescued rMACV replicated in a fashion similar to that of its parental wild-type MACV in cultured cells.

***In vivo* characterization of Machupo virus in IFN- $\alpha\beta/\gamma$ R^{-/-} mice.** To examine and compare the disease development and pathogenesis caused by the parental and recombinant MACV *in vivo*, two experiments were completed in which C57BL/6 IFN-

$\alpha\beta/\gamma$ R^{-/-} ($n = 26$) and wild-type C57BL/6 mice ($n = 10$) were challenged i.p. with 1×10^4 PFU of MACV or rMACV. Two IFN- $\alpha\beta/\gamma$ R^{-/-} mice were mock infected as the negative control. Changes in temperature and body weight were observed throughout the study. From 10 to 14 dpi, significant weight loss ($P < 0.05$) was identified in the infected IFN- $\alpha\beta/\gamma$ R^{-/-} mice compared to the infected wild-type mice and the uninfected control mice (Fig. 4A). At 20 dpi, neurological impairment, including partial paralysis, hunched posture, labored breathing, and awkward gait were observed in IFN- $\alpha\beta/\gamma$ R^{-/-} mice infected with MACV and rMACV. In contrast, the wild-type mice infected by either wild-type MACV or rMACV did not exhibit any observable symptoms.

From 1 to 20 dpi, no significant change in temperature was observed among any of the groups of mice (Fig. 4B). Starting at 22 dpi, the infected IFN- $\alpha\beta/\gamma$ R^{-/-} mice began succumbing to infection (Fig. 4C). Weight loss and temperature loss were observed 1 to 2 days prior to death (Fig. 4C). The mortality rate for both viruses was 92.8%, with an average time to death of 28.6 dpi. There was no significant difference in the mean time to death between the two viruses ($P > 0.35$).

Titration of brain homogenate confirmed similar viral load between rMACV- and MACV-infected animals, with the highest virus titer observed at 24 dpi. A high viral load ($\sim 10^7$ PFU/gram) was found in the brains of infected IFN- $\alpha\beta/\gamma$ R^{-/-} mice, which was maintained until death (Fig. 5A). The single surviving mouse, which was infected with MACV and was euthanized at 40 dpi, had no detectable viral load in the brain (data not shown). Titrations

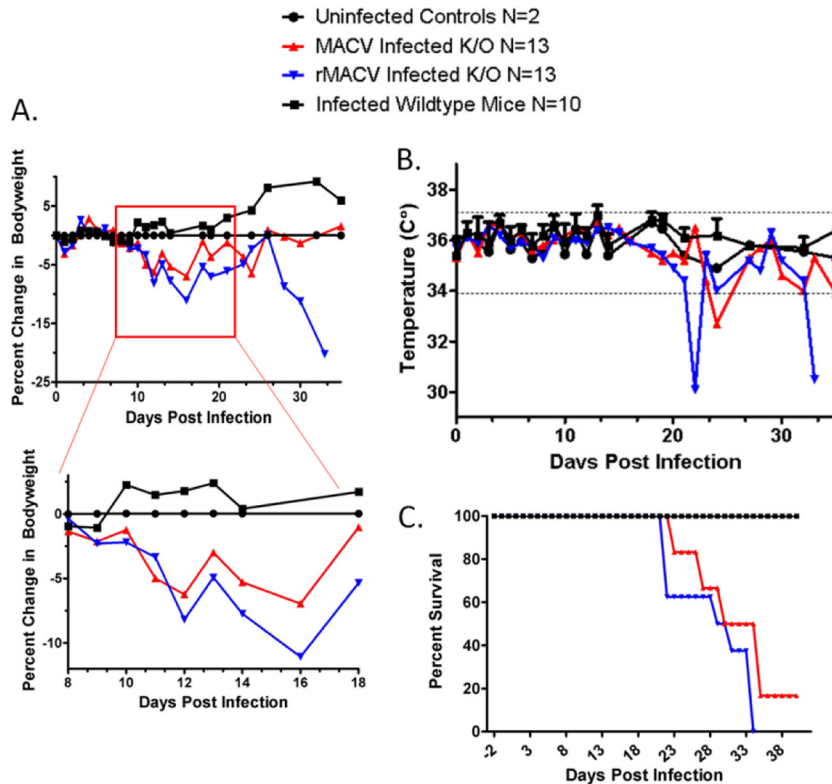


FIG 4 Infection of IFN- $\alpha\beta/\gamma$ R^{-/-} mice with MACV and rMACV. Twenty-eight IFN- $\alpha\beta/\gamma$ R^{-/-} mice and 10 wild-type C57BL/6 mice were either mock infected or challenged intraperitoneally with MACV or rMACV (1×10^4 PFU). Scheduled euthanizing occurred at 14 dpi and 24 dpi following weight loss and neurological disease development. (A) Weight changes. A biphasic disease can be identified through analysis of body weight loss. From 10 to 14 dpi, significant weight loss ($P < 0.05$) can be identified between the MACV- or rMACV-infected IFN- $\alpha\beta/\gamma$ R^{-/-} mice and the wild-type mice. Additional weight loss after the acute phase was identified in animals 1 to 2 days before they succumbed to the disease. No difference was identified in weight loss between MACV- and rMACV-infected animals prior to the final stages of succumbing to the disease. (B) Body temperature changes. There was no detectable development of hyperthermia during the acute phase of the disease. Severe temperature loss was observed 1 to 2 days prior to succumbing to disease. (C) Animal survival after virus infection. Animals allowed to fully progress in disease development ($n = 6$ for MACV, $n = 8$ for rMACV) showed significant neurological impairment identified at 20 dpi. All animals infected with rMACV died or were euthanized when they reached the disease endpoint by 34 dpi. One MACV-infected animal survived to the end of the study at 40 dpi.

of spleen homogenates from infected IFN- $\alpha\beta/\gamma$ R^{-/-} mice collected on the same days showed a high viral load at 14 dpi with a slight decline at 24 and 30 to 34 dpi (Fig. 5B). Titration of serum samples revealed a trend of decreased viremia from 14 dpi (Fig. 5C).

Histopathology analysis of tissues from infected IFN- $\alpha\beta/\gamma$ R^{-/-} mice demonstrated increasing neuronal damage starting at 14 dpi up to death along with minor vascular and perivascular mononuclear infiltrates in the cortex of the brain (Fig. 6, panels II, III, and IV). The spleen of IFN- $\alpha\beta/\gamma$ R^{-/-} mice infected with MACV or rMACV showed prominent alterations in microarchitecture with an increase in white pulp volume and expansion of the periarteriolar lymphoid sheath (Fig. 6, panels VIII, IX, and X). The spleen of the wild-type mice infected with MACV and the uninfected IFN- $\alpha\beta/\gamma$ R^{-/-} mice showed normal white pulp architectures (Fig. 6, panels VI to VII). Further experimentation is ongoing to better characterize this novel model for studying Machupo infection *in vivo* and to elucidate the mechanisms for the late neurological disease.

DISCUSSION

Our MACV sequencing result clearly shows that the terminal 19-nucleotide sequences at the 5' and 3' UTRs are different from

those previously reported in the GenBank. Compared to our new data, the MACV sequences available from GenBank (JN794584 and AY619643) have the C6A and G8U substitutions at the 5' end of the S segment, which predict a perfect base pairing between the 5' and 3' ends of the S segment. Our new data suggested two mismatches at positions 6 and 8 in the same region (Fig. 1B), which is consistent with the sequences of other arenaviruses such as JUNV and LASV (42, 45, 46). The terminal 19 nucleotides at the 5' and 3' ends of L and S genomic RNAs are highly conserved among arenaviruses and play critical roles in viral RNA replication and transcription. Although mutations in positions 6 and 8 are relatively better tolerated than changes in other positions, a previous study using an LASV minireplicon system has demonstrated that the same C6A and G8U mutations at the 5' end of S genomic RNA greatly inhibit LASV viral gene expression by 60% and 90%, respectively (45). For JUNV, RNA sequences with the same C6A and G8U substitutions at the 5' terminus of S segment were reported in GenBank (AY619641) and were determined to be non-functional for the rescue of a recombinant JUNV strain (42). Our attempts to rescue MACV with UTRs different from our identified sequence were unsuccessful (data not shown), highlighting the critical role of these highly conserved sequences at the 5' and 3'

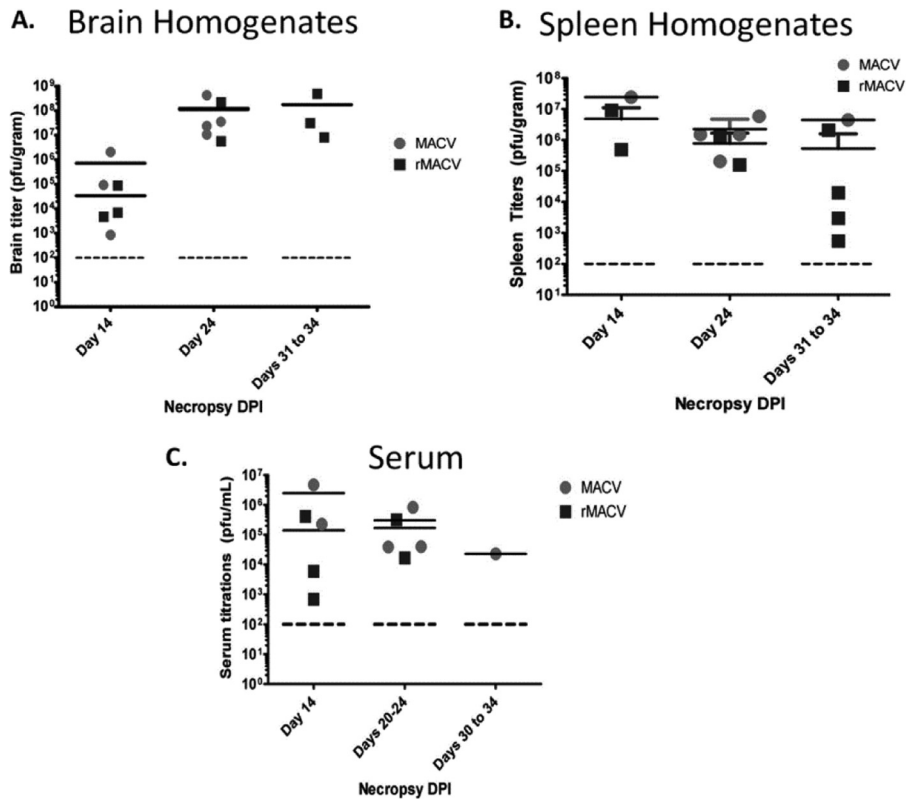


FIG 5 Virus titers in organs of infected IFN- $\alpha\beta/\gamma$ R^{-/-} mice. Dotted lines represent the minimal virus load that can be detected. (A) Virus titers of brain homogenates collected from infected IFN- $\alpha\beta/\gamma$ R^{-/-} mice at 14, 24, and 31 to 34 dpi. Viral load for rMACV and MACV are similar at 24 and 30 to 34 dpi. Peak viral load correlates with onset of neurological disease. (B) Viral load in spleen homogenates. (C) Viremia in serum samples collected at 14, 20 to 24, and 30 to 34 dpi.

termini of viral genomic RNA in viral replication. Additionally, a previous study showed the important role of the 3' terminal sequence of the MACV S segment in MACV RNA polymerase recruitment (44).

The MG was utilized to confirm that the MACV L protein and NP were sufficient to support efficient viral RNA transcription

and replication of the MACV MG genome. The establishment of an MACV-derived MG will provide an additional tool to study the molecular biology of new world arenaviruses. MG systems of other arenaviruses have been proven to be useful tools in dissecting the role of viral proteins in arenavirus RNA replication and transcription, identifying the function of the IGR as the transcrip-

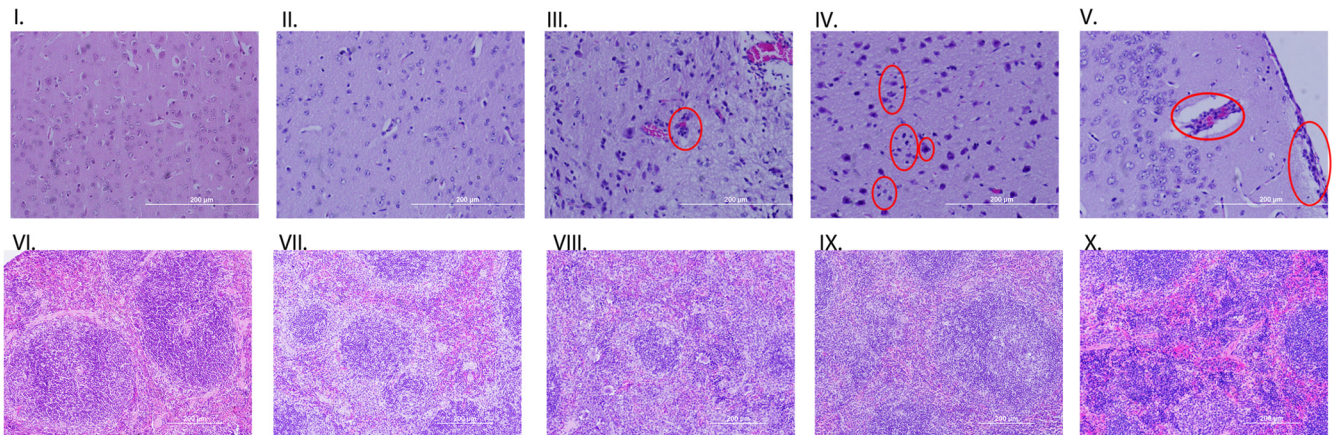


FIG 6 Histopathology staining of brain and spleen tissues. Sections I and VI are from an uninfected IFN- $\alpha\beta/\gamma$ R^{-/-} mouse showing no neuronal death and good spleen structure. Sections II and VII are from a C57BL/6 mouse infected with MACV with no visible neuron death or inflammation and good spleen structure. Sections III and VIII are from an IFN- $\alpha\beta/\gamma$ R^{-/-} mouse euthanized at 14 dpi, the red circle identifying vascular infiltrates. Sections IV and IX are from an IFN- $\alpha\beta/\gamma$ R^{-/-} euthanized at 24 dpi; red circles identify microglial cells and cellular debris from dead neuronal cells. Sections V and X are from an IFN- $\alpha\beta/\gamma$ R^{-/-} mouse that died at 34 dpi; red circles identify increased vascular and perivascular cellular infiltrates.

tion terminating signal, studying the role of Z as a matrix protein, and mapping the cap snatching domain of L protein (47–52). The development of an MG for MACV may assist in studying the replication of this virus in the BSL-2 environment, which may also be utilized as a tool for testing antivirals as it has been shown for the Lassa virus MG system (53).

Our studies also provided preliminary evidence for the compatibility of Candid #1 L protein and NP for supporting MACV RNA template replication. This evidence, in combination with the availability of the reverse genetics system, will allow for the generation of chimeric viruses containing genetic sequences from both MACV and Candid #1. The generation of a Lassa/Mopeia reassortment virus as a method of attenuation has been proven effective with Old World arenaviruses, but never with New World arenaviruses (54). We propose the introduction of an attenuating sequence or replacement of entire genes from Candid #1 into the MACV backbone, which may allow for the rational generation of a live-attenuated vaccine candidate for MACV. Our *in vitro* studies have proved similar growth patterns for wild-type MACV and rMACV. Furthermore, *in vivo* studies provide additional evidence that rMACV is similar to MACV. Challenge with rMACV and MACV led to similar disease development, weight loss, neurological symptoms, and death in IFN- $\alpha\beta/\gamma$ R^{-/-} mice. Viral invasion of the brain appears to have occurred in a similar manner in both groups of mice, with comparable peak viral loads at 24 dpi. The findings in this study, utilizing the IFN- $\alpha\beta/\gamma$ R^{-/-} mice, identified the development of a biphasic disease with an acute weight loss occurring between 9 and 14 dpi and LNS between 20 and 34 dpi. Previously, a lethal model of MACV infection was reported using STAT-1^{-/-} adult mice, which succumb rapidly to disease without developing LNS (33). However, the biphasic disease described in this study is similar to some of the reports of BHF in humans as well as in multiple species of NHPs experimentally infected with MACV (35, 36, 55, 56). The neurological disease in the late stages of BHF in humans can be correlated to the development of awkward gait, labored breathing, and partial paralysis observed in our murine model (16, 19). In NHPs, LNS has been reported in multiple species with mortality near 100%, which is highly comparable to the IFN- $\alpha\beta/\gamma$ R^{-/-} model reported here.

One of the most common complications in humans after infection with various hemorrhagic arenaviruses, including Machupo and Junin viruses, is the presence of LNS, which can be lethal or result in transient or permanent neurological sequelae (57, 58). In addition, a portion of patients who have recovered from Lassa fever develop a long-term hearing loss, showing a potential neurological impact of Old World arenaviruses. The mechanism for disease development in MACV-infected IFN receptor knockout mice, but not in the parental wild-type mice, is still unclear, which certainly warrants future studies. We believe that our novel murine model can become a very useful tool to study the neurological syndrome caused by MACV and potentially other arenaviruses. The experimental development of neurological disease for MACV has been described only in NHPs so far, which are costly and not easy to handle in the BSL-4 laboratory. Utilizing mice instead of NHPs for neurological disease modeling has multiple benefits. For example, many immunological and imaging tools are available for further elucidation of neurological disease development, and working with mice in the BSL-4 environment is considered to be safer, faster, and more cost-effective than research with NHPs.

The lack of any disease development in the wild-type C57BL/7

mice corresponds to previously reported data. The lack of weight loss and the 100% survival rate compared to the IFN- $\alpha\beta/\gamma$ R^{-/-} mice suggests a potential and important role that the innate immune response plays in BHF development, which will need to be further elucidated.

Taken together, this paper has identified the functional 19-nucleotide sequences at the 5' and 3' ends of the MACV S and L genomic RNAs. We have generated an MG system for analyzing the replication and transcription of both the S and L segments of the MACV template. This new system was used to demonstrate the compatibility of L and NP between MACV and two different Junin viruses. We also believe that the establishment of MGs allows for future vaccine and antiviral studies in the BSL-2 laboratory. Additionally, we have successfully rescued rMACV and have reported *in vitro* characterization of its growth in Vero and A549 cells. Following challenge in IFN- $\alpha\beta/\gamma$ R^{-/-} mice, we have also identified the first murine model for MACV-induced LNS, which is similar to the biphasic disease reported in human cases and NHP studies.

ACKNOWLEDGMENTS

This research was supported by funding in part through the National Institute of Allergy and Infectious Diseases Public Health Service grant UC7AI094660, Public Health Service grant R01AI093445, the University of Texas Medical Branch Institute for Translational Sciences (NCRR RR029876), and the University of Texas Medical Branch Institute for Human Infections and Immunity. The funders had no role in study design, data collection and analysis, decision to publish, or preparation of the manuscript.

REFERENCES

1. Beyer WR, Pöplau D, Garten W, von Laer D, Lenz O. 2003. Endoproteolytic processing of the lymphocytic choriomeningitis virus glycoprotein by the subtilase SKI-1/SIP. *J. Virol.* 77:2866–2872. <http://dx.doi.org/10.1128/JVI.77.5.2866-2872.2003>.
2. York J, Romanowski V, Lu M, Nunberg JH. 2004. The signal peptide of the Junin arenavirus envelope glycoprotein is myristoylated and forms an essential subunit of the mature G1-G2 complex. *J. Virol.* 78:10783–10792. <http://dx.doi.org/10.1128/JVI.78.19.10783-10792.2004>.
3. Eichler R, Lenz O, Strecker T, Eickmann M, Klenk H-D, Garten W. 2003. Identification of Lassa virus glycoprotein signal peptide as a trans-acting maturation factor. *EMBO Rep.* 4:1084–1088. <http://dx.doi.org/10.1038/sj.embor.7400002>.
4. York J, Nunberg JH. 2006. Role of the stable signal peptide of Junin arenavirus envelope glycoprotein in pH-dependent membrane fusion. *J. Virol.* 80:7775–7780. <http://dx.doi.org/10.1128/JVI.00642-06>.
5. Strecker T, Eichler R, Meulen Jt, Weissenhorn W, Dieter Klenk H, Garten W, Lenz O. 2003. Lassa virus Z protein is a matrix protein sufficient for the release of virus-like particles. *J. Virol.* 77:10700–10705. <http://dx.doi.org/10.1128/JVI.77.19.10700-10705.2003>.
6. Meyer BJ, Southern PJ. 1994. Sequence heterogeneity in the termini of lymphocytic choriomeningitis virus genomic and antigenomic RNAs. *J. Virol.* 68:7659–7664.
7. Tortorici MA, Albarino CG, Posik DM, Ghiringhelli PD, Lozano ME, Rivera Pomar R, Romanowski V. 2001. Arenavirus nucleocapsid protein displays a transcriptional antitermination activity *in vivo*. *Virus Res.* 73:41–55. [http://dx.doi.org/10.1016/S0168-1702\(00\)00222-7](http://dx.doi.org/10.1016/S0168-1702(00)00222-7).
8. Mackenzie RB, Beye HK, Valverde L, Garron H. 1964. Epidemic hemorrhagic fever in Bolivia. I. A preliminary report of the epidemiologic and clinical findings in a new epidemic area in South America. *Am. J. Trop. Med. Hyg.* 13:620–625.
9. Webb PA. 1965. Properties of Machupo virus. *Am. J. Trop. Med. Hyg.* 14:799–802.
10. Johnson KM, Wiebenga NH, Mackenzie RB, Kuns ML, Tauraso NM, Shelokov A, Webb PA, Justines G, Beye HK. 1965. Virus isolations from human cases of hemorrhagic fever in Bolivia. *Proc. Soc. Exp. Biol. Med. (New York, NY)* 118:113–118. <http://dx.doi.org/10.3181/00379727-118-29772>.

11. Kuns ML. 1965. Epidemiology of Machupo virus infection. *Am. J. Trop. Med. Hyg.* 14:813–816.
12. Delgado S, Erickson BR, Agudo R, Blair PJ, Vallejo E, Albariño CG, Vargas J, Comer JA, Rollin PE, Ksiazek TG, Olson JG, Nichol ST. 2008. Chapare virus, a newly discovered arenavirus isolated from a fatal hemorrhagic fever case in Bolivia. *PLoS Pathog.* 4:e1000047. <http://dx.doi.org/10.1371/journal.ppat.1000047>.
13. Peters CJ. 2002. Human infection with arenaviruses in the Americas. *Curr. Top. Microbiol. Immunol.* 262:65–74.
14. Harrison LH, Halsey NA, McKee KT, Jr, Peters CJ, Barrera Oro JG, Briggiler AM, Feuillade MR, Maiztegui JI. 1999. Clinical case definitions for Argentine hemorrhagic fever. *Clin. Infect. Dis.* 28:1091–1094. <http://dx.doi.org/10.1086/514749>.
15. Weissenbacher MC, Laguens RP, Coto CE. 1987. Argentine hemorrhagic fever. *Curr. Top. Microbiol. Immunol.* 134:79–116.
16. Stinebaugh BJ, Schloeder FX, Johnson KM, Mackenzie RB, Entwisle G, De Alba E. 1966. Bolivian hemorrhagic fever: a report of four cases. *Am. J. Med.* 40:217–230. [http://dx.doi.org/10.1016/0002-9343\(66\)90103-3](http://dx.doi.org/10.1016/0002-9343(66)90103-3).
17. Kilgore PE, Peters CJ, Mills JN, Rollin PE, LA, Khan AS, Ksiazek TG. 1995. Prospects for the control of Bolivian hemorrhagic fever. *Emerg. Infect. Dis.* 1:97–100. <http://dx.doi.org/10.3201/eid0103.950308>.
18. Webb PA, Johnson KM, Mackenzie RB, Kuns ML. 1967. Some characteristics of Machupo virus, causative agent of Bolivian hemorrhagic fever. *Am. J. Trop. Med. Hyg.* 16:531–538.
19. Child PL, MacKenzie RB, Valverde LR, Johnson KM. 1967. Bolivian hemorrhagic fever. A pathologic description. *Arch. Pathol.* 83:434–445.
20. Johnson KM, Kuns ML, Mackenzie RB, Webb PA, Yunker CE. 1966. Isolation of Machupo virus from wild rodent *Calomys callosus*. *Am. J. Trop. Med. Hyg.* 15:103–106.
21. Kilgore PE, Ksiazek TG, Rollin PE, Mills JN, Villagra MR, Montenegro MJ, Costales MA, Paredes LC, Peters CJ. 1997. Treatment of Bolivian hemorrhagic fever with intravenous ribavirin. *Clin. Infect. Dis.* 24:718–722. <http://dx.doi.org/10.1093/clind/24.4.718>.
22. Peters CJ, Kuehne RW, Mercado RR, Le Bow RH, Spertzel RO, Webb PA. 1974. Hemorrhagic fever in Cochabamba, Bolivia, 1971. *Am. J. Epidemiol.* 99:425–433.
23. Aguilar PV, Camargo W, Vargas J, Guevara C, Roca Y, Felices V, Laguna-Torres A, Tesh R, Ksiazek TG, Kochel TJ. September 2009, posting date. Reemergence of Bolivian hemorrhagic fever, 2007–2008. (Letter.) <http://dx.doi.org/10.3201/eid159.090017>.
24. ProMED-email. 2013. Bolivian hemorrhagic fever—Bolivia: (BENI). ProMED-email 20130317.1590121. <http://www.promedmail.org/direct.php?id=20130317.1590121>.
25. ProMED-email. 2013. Bolivian hemorrhagic fever—Bolivia (02): (BE). ProMED-email 20130420.1660132. <http://www.promedmail.org/direct.php?id=20130420.1660132>.
26. ProMED-email. 2012. Bolivian hemorrhagic fever—Bolivia (05): (BENI). ProMED-email 20120730.1220842. <http://www.promedmail.org/direct.php?id=20120730.1220842>.
27. ProMED-email. 2011. Bolivian hemorrhagic fever—Bolivia: (BE). ProMED-email 20111202.3514. <http://www.promedmail.org/direct.php?id=20111202.3514>.
28. Buchmeier M, de la Torre J, Peters C. 2007. Arenaviridae: the viruses and their replication, p 1791–1827. *In* Knipe DM, Howley PM, Griffin DE, Lamb RA, Martin MA, Roizman B, Straus SE (ed), *Fields virology*, 5th ed. Lippincott Williams & Wilkins, Philadelphia, PA.
29. Eddy G, Wagner F, Scott S, Mahlandt B. 1975. Protection of monkeys against Machupo virus by the passive administration of Bolivian haemorrhagic fever immunoglobulin (human origin). *Bull. World Health Organ.* 52:723–727.
30. Stephen EL, Scott SK, Eddy GA, Levy HB. 1977. Effect of interferon on togavirus and arenavirus infections of animals. *Texas Rep. Biol. Med.* 35:449–454.
31. Jahrling P, Trotter R, Barrero O. 1988. Cross protection against Machupo with candid #1 Junin virus vaccine. Oral presentation. Proceedings of the Second International Conference on the Impact of Viral Diseases on the Development of Latin American Countries and the Caribbean Region. Mar del Plata, Argentina.
32. Maiztegui JI, McKee KT, Jr, Barrera Oro JG, Harrison LH, Gibbs PH, Feuillade MR, Enria DA, Briggiler AM, Levis SC, Ambrosio AM, Halsey NA, Peters CJ. 1998. Protective efficacy of a live attenuated vaccine against Argentine hemorrhagic fever. *AHF Study Group. J. Infect. Dis.* 177:277–283. <http://dx.doi.org/10.1086/514211>.
33. Bradfute S, Stuthman K, Shurtleff A, Bavari S. 2011. A STAT-1 knock-out mouse model for Machupo virus pathogenesis. *Virol. J.* 8:300. <http://dx.doi.org/10.1186/1743-422X-8-300>.
34. McLeod CG, Stookey JL, Eddy GA, Scott K. 1976. Pathology of chronic Bolivian hemorrhagic fever in the rhesus monkey. *Am. J. Pathol.* 84:211–224.
35. Castello MD, Eddy GA, Kuehne RW. 1976. A rhesus monkey model for the study of Bolivian hemorrhagic fever. *J. Infect. Dis.* 133:57–62. <http://dx.doi.org/10.1093/infdis/133.1.57>.
36. McLeod CG, Stookey JL, White JD, Eddy GA, Fry GA. 1978. Pathology of Bolivian hemorrhagic fever in the African green monkey. *Am. J. Trop. Med. Hyg.* 27:822–826.
37. Kenyon RH, Green DE, Eddy GA, Peters CJ. 1986. Treatment of Junin virus-infected guinea pigs with immune serum: development of late neurological disease. *J. Med. Virol.* 20:207–218. <http://dx.doi.org/10.1002/jmv.1890200303>.
38. Kolokoltsova OA, Yun NE, Poussard AL, Smith JK, Smith JN, Salazar M, Walker A, Tseng C-TK, Aronson JF, Paessler S. 2010. Mice lacking alpha/beta and gamma interferon receptors are susceptible to Junin virus infection. *J. Virol.* 84:13063–13067. <http://dx.doi.org/10.1128/JVI.01389-10>.
39. Maiztegui JI, Fernandez NJ, de Damilano AJ. 1979. Efficacy of immune plasma in treatment of Argentine haemorrhagic fever and association between treatment and a late neurological syndrome. *Lancet* ii:1216–1217.
40. Johnson KM, McCormick JB, Webb PA, Smith ES, Elliott LH, King JJ. 1987. Clinical virology of Lassa fever in hospitalized patients. *J. Infect. Dis.* 155:456–464. <http://dx.doi.org/10.1093/infdis/155.3.456>.
41. McCormick JB, Fisher-Hoch SP. 2002. Lassa fever. *Curr. Top. Microbiol. Immunol.* 262:75–109.
42. Emonet SF, Seregin AV, Yun NE, Poussard AL, Walker AG, de la Torre JC, Paessler S. 2011. Rescue from cloned cDNAs and *in vivo* characterization of recombinant pathogenic Romero and life-attenuated Candid #1 strains of Junin virus, the causative agent of Argentine hemorrhagic fever disease. *J. Virol.* 85:1473–1483.
43. Bergeron É, Chakrabarti AK, Bird BH, Dodd KA, McMullan LK, Spiropoulos CF, Nichol ST, Albariño CG. 2012. Reverse genetics recovery of Lujo Virus and role of virus RNA secondary structures in efficient virus growth. *J. Virol.* 86:10759–10765. <http://dx.doi.org/10.1128/JVI.01144-12>.
44. Kranzusch PJ, Schenk AD, Rahmeh AA, Radoshitzky SR, Bavari S, Walz T, Whelan SP. 2010. Assembly of a functional Machupo virus polymerase complex. *Proc. Natl. Acad. Sci. U. S. A.* 107:20069–20074. <http://dx.doi.org/10.1073/pnas.1007152107>.
45. Hass M, Westerkofsky M, Müller S, Becker-Ziaja B, Busch C, Günther S. 2006. Mutational analysis of the Lassa virus promoter. *J. Virol.* 80:12414–12419. <http://dx.doi.org/10.1128/JVI.01374-06>.
46. Albariño CG, Bergeron É, Erickson BR, Khristova ML, Rollin PE, Nichol ST. 2009. Efficient reverse genetics generation of infectious Junin viruses differing in glycoprotein processing. *J. Virol.* 83:5606–5614. <http://dx.doi.org/10.1128/JVI.00276-09>.
47. Cornu TI, de la Torre JC. 2001. RING finger Z protein of lymphocytic choriomeningitis virus (LCMV) inhibits transcription and RNA replication of an LCMV S-segment minigenome. *J. Virol.* 75:9415–9426. <http://dx.doi.org/10.1128/JVI.75.19.9415-9426.2001>.
48. Hass M, Golnitz U, Muller S, Becker-Ziaja B, Gunther S. 2004. Replicon system for Lassa virus. *J. Virol.* 78:13793–13803. <http://dx.doi.org/10.1128/JVI.78.24.13793-13803.2004>.
49. Lee KJ, Novella IS, Teng MN, Oldstone MB, de La Torre JC. 2000. NP and L proteins of lymphocytic choriomeningitis virus (LCMV) are sufficient for efficient transcription and replication of LCMV genomic RNA analogs. *J. Virol.* 74:3470–3477. <http://dx.doi.org/10.1128/JVI.74.8.3470-3477.2000>.
50. Lopez N, Jacamo R, Franze-Fernandez MT. 2001. Transcription and RNA replication of Tacaribe virus genome and antigenome analogs require N and L proteins: Z protein is an inhibitor of these processes. *J. Virol.* 75:12241–12251. <http://dx.doi.org/10.1128/JVI.75.24.12241-12251.2001>.
51. Pinschewer DD, Perez M, de la Torre JC. 2005. Dual role of the lymphocytic choriomeningitis virus intergenic region in transcription termination and virus propagation. *J. Virol.* 79:4519–4526. <http://dx.doi.org/10.1128/JVI.79.7.4519-4526.2005>.
52. Lelke M, Brunotte L, Busch C, Gunther S. 2010. An N-terminal region of Lassa virus L protein plays a critical role in transcription but not replication of the virus genome. *J. Virol.* 84:1934–1944. <http://dx.doi.org/10.1128/JVI.01657-09>.
53. Muller S, Gunther S. 2007. Broad-spectrum antiviral activity of small

- interfering RNA targeting the conserved RNA termini of Lassa virus. *Antimicrob. Agents Chemother.* 51:2215–2218. <http://dx.doi.org/10.1128/AAC.01368-06>.
54. Lukashevich IS, Patterson J, Carrion R, Moshkoff D, Ticer A, Zapata J, Brasky K, Geiger R, Hubbard GB, Bryant J, Salvato MS. 2005. A live attenuated vaccine for Lassa fever made by reassortment of Lassa and Mopeia viruses. *J. Virol.* 79:13934–13942. <http://dx.doi.org/10.1128/JVI.79.22.13934-13942.2005>.
55. Webb PA, Justines G, Johnson KM. 1975. Infection of wild and laboratory animals with Machupo and Latino viruses. *Bull. World Health Organ.* 52:493–499.
56. Eddy G, Scott S, Wagner F, Brand O. 1975. Pathogenesis of Machupo virus infection in primates. *Bull. World Health Organ.* 52:517–521.
57. Grant A, Seregin A, Huang C, Kolokoltsova O, Brasier A, Peters C, Paessler S. 2012. Junin virus pathogenesis and virus replication. *Viruses* 4:2317–2339. <http://dx.doi.org/10.3390/v4102317>.
58. Yun NE, Walker DH. 2012. Pathogenesis of Lassa fever. *Viruses* 4:2031–2048. <http://dx.doi.org/10.3390/v4102031>.